

NUCLEATION OF MARTENSITE IN IRON BASE ALLOYS

BY

AMARAVADI V. ANANDASWAROOP

~~CHIT~~

ME

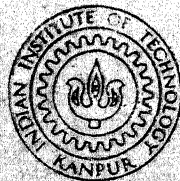
1968

10

ANA

NUC

TH
ME/1968/1m
An 14 n.



DEPARTMENT OF METALLURGICAL ENGINEERING

INDIAN INSTITUTE OF TECHNOLOGY KANPUR

M.Tech

CENTRAL LIBRARY
Indian Institute of Technology
KANPUR

Class No... *Thesis*
669-1
An 14 n

NUCLEATION OF MARTENSITE

IN IRON BASE ALLOYS

THESIS

Submitted in Partial Fulfillment
of the Requirements for the
Degree of

Master of Technology (Metallurgical Engineering)

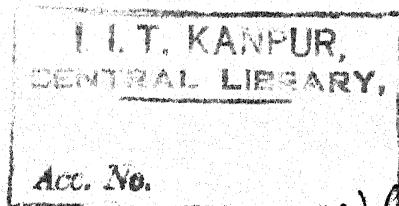
at the

INDIAN INSTITUTE OF TECHNOLOGY, KANPUR

by

Amaravadi V. Anandaswaroop

September 1968



*Thesis
669.1
An 14 m*

ME-1968-PA ANA-NV

Approved:

Raghavan

Thesis Advisor

K.P. J.

Head of the Department

ACKNOWLEDGEMENTS

The author wishes to express his deep sense of gratitude to Dr.V.Raghavan for introducing him to the field of martensite transformations. Special thanks are due to him for his guidance and encouragement.

The author thanks the staff of the Precision Shop and the Low Temperature Laboratory for their cooperation. Thanks are due to Mr.K.P.Mukherji and Mr.M.Pandey for their help in arranging the experiments.

SUMMARY

The literature on the kinetics of the martensite transformation in iron base alloys is reviewed with special reference to the nucleation of martensite.

Austenitized specimens of Fe-30% Ni alloys are quenched to -95°C and after 3 minutes of isothermal holding they are upquenched to various holding temperatures between -80°C and -10°C at ten degree intervals. Percentage of martensite formed verses time curves are obtained from electrical resistance measurements. A Kelvin bridge is used for the electrical resistance measurements.

The ratio of the transformation rates just after and before the upquench is taken as the ratio of the nucleation rates at the two temperatures. Activation energy is found to be proportional to the driving^{force} for the transformation. Nucleation rates show a C-curve behaviour and the temperature at which maximum nucleation rate occurs is around 72°C . The size of the embryo and the interfacial energy of the embryo are calculated to give best fit with the Kaufman-Cohen model of the martensite embryo. Kaufman-Cohen model predicts that the activation energy at any temperature is maximum for a size r_+ and for embryos smaller than r_+ the activation energy is proportional to $\sqrt{\text{(driving force)}}$ while it is directly proportional to the driving force for embryos larger than r_+ . But the calculated size of the embryo is smaller than r_+ . To explain the observed proportionality between activation energy and the driving force, it is argued that the value of r_+ is lowered by the

-3

strains produced in the matrix during the transformation. Considering the effect of transformation strains on the energetics of the martensite embryo, it is shown that the increase in the number of operative embryos is proportional to the volume fraction of martensite formed, and the thickness to length ratio of martensite plates is larger for the plates that form at later stages of the transformation. The discrepancy at later stages of the transformation between the experimentally determined transformation curves and the curves calculated on the basis of a theoretical model by Raghavan is qualitatively explained to be due to the lowering of the activation energy due to the transformation strains.

CONTENTS

Page No.

SUMMARY

1. LITERATURE REVIEW

1.1 Introduction	1
1.2 Essential Kinetic Features	1
1.3 Evidence for Heterogeneous Nucleation	4
1.4 The Reaction Path Model	5
1.5 The Dislocation Model of Martensite Embryo	8
1.6 Experimental Validity of the Dislocation Model	13
1.7 Geometry of Martensite Units	16
1.8 Autocatalysis	17

2. THE EXPERIMENTAL DETAILS

2.1 Preparation of the Specimen	19
2.2 Austenitizing Treatment	19
2.3 Electropolishing	20
2.4 The Kelvin Bridge	21
2.5 The Experimental Procedure	22
2.6 Calculation of Percentage Martensite	23

3. RESULTS AND DISCUSSION

3.1 Introduction	27
3.2 The C-curve Behaviour	29
3.3 Activation Energy Proportional to the Driving Force	32
3.4 Calculations with the Data from Machlin and Cohen	33
3.5 The Effect of Strains in the Matrix on Nucleation	36

4. CONCLUSIONS	40
----------------	----

TABLE I

APPENDIX I

REFERENCES

1. LITERATURE REVIEW

1.1 Introduction:

Martensite has very high technological significance since it is the hardest phase in steels. The structure and properties of martensite are manifested through the diffusionless nature of the transformation. The control of the transformation for better properties can be achieved if the nature and mechanism of the transformation are well understood. Unfortunately the progress of the martensitic transformation is not yet fully known. A brief review of the present day concepts on the kinetics of martensite transformation is presented in this chapter.

1.2 Essential Kinetic Features:

There are three types of martensite transformations which can be distinguished by their kinetics. In most of the alloys, the transformation shows athermal nature. As soon as the material is quenched to a temperature in the transformation range, a definite amount of martensite characteristic of the temperature forms within a very short interval of time. No further transformation occurs even after long periods of isothermal holding.

Iron-nickel and iron-nickel-carbon alloys with M_s below room temperature show discontinuous transformation curves. A relatively large amount of martensite forms in

a very short interval of time and may be followed by a small amount of isothermal transformation. Austenite does not transform at temperatures even slightly higher than M_s , but a large amount of martensite forms at the M_s temperature.

Certain alloys with M_s below room temperature undergo completely isothermal transformation. Fe - Ni - Mn, Fe - Ni - Mn - C, Fe - 2.55 Cr - 0.11 Ni - 0.22 Mn - 1.43 C alloys are some examples. Initially the transformation rate is slow and after a small amount of transformation the rate quickly increases. At a later stage, the transformation rate falls off gradually. After certain time the amount of martensite remains almost constant. The final amount depends upon the temperature of the transformation.

Philibert and Grussard¹ slowed down by a stabilization treatment the rate of the transformation in a Fe - Cr - C alloy which would have been athermal otherwise, and observed the isothermal transformation with an incubation period. Their results suggest that the nature of the transformation may be the same for the three types of transformation; the differences in kinetics may be only in the magnitude of the transformation rate. In all the three types of transformation, the final amount of martensite is a function of temperature. They differ only on time scale.

The formation of martensite involves a rapid movement of the interface separating martensite and austenite. As the

interface advances into austenite, atoms from the austenite phase are transferred across the interface into the martensite phase. Bunshah and Mehl² determined the propagation rate of the interface to be about 10^5 cm/sec in Fe - 29.5% Ni alloy. This is about one third the velocity of sound and is independent of the temperature over the range of -20°C to -195°C . With this high rate of propagation, a full size plate of martensite forms in $0.05 - 0.5 \mu\text{-sec}$. These experiments show that the growth of martensite is not a thermally activated process. It is also evident that the interface separating austenite and martensite must be highly mobile.

As soon as a nucleus is created, it grows to the final size, and there is no further growth even if the driving force for transformation is increased by lowering the temperature. Since growth to the final size takes practically zero time, the kinetics are entirely determined by the nucleation events. These observations hold good for all the three types of martensite transformations. The transformation does not take place at the temperature at which the free energy difference between austenite and martensite is zero; but occurs only at temperatures at which there is sufficient driving force for the nucleation process.

Cech and Hollomon³ have shown that the isothermal kinetics in Fe - Ni - Mn alloy show a C-curve behaviour on

Fig 1-1

T - T - T diagram. The maximum rate of transformation is found in the vicinity of 100 - 150°K. The transformation can be suppressed⁴ by rapid cooling to 4°K, but transformation takes place if the specimen is heated up from 4°K to a temperature below M_s . These results suggest that the nucleation is a thermally activated process.

1.3 Evidence for Heterogeneous Nucleation:

Cech and Turnbull⁵ austenitized tiny particles of an Fe - Ni alloy and quenched into the martensite temperature range. Different particles transformed at different temperatures and some did not transform at all even at very low temperatures. The conclusion obviously was that the nucleation was heterogeneous. The particles that did not contain the preferred sites for nucleation did not transform.

Metallographic observations show that the position and formation sequence of martensite plates on cooling is repeated exactly in the next cooling cycle after reversal of the transformation by heating. In gold - 47.5 at% cadmium, high austenitizing temperatures and times reduce the number of nucleating sites. Therefore, it can be concluded that martensite forms only at preferred sites.

Fisher et al suggested that these preferred sites might be composition fluctuations. A statistical distribution of such composition fluctuations is supposed to be equilibrium

at the austenitizing temperature. Such composition fluctuations are frozen in during the quenching and they act as nucleation sites. But the concept of such statistical distribution should lead to the presence of such fluctuations at random and the reproducibility of the formation sequence of the martensite plates in a given specimen on reverses of transformation cannot be explained.

The other alternative can be structural heterogeneities, consisting of non-equilibrium lattice imperfections, internal surfaces and local strains due to accidents of crystal growth or plastic deformation. The exact nature of the nucleation sites is not yet known. Two models are discussed here, both of them assume the pre-existence of the embryos in the austenite.

1.4 The Reaction Path Model:

A small region in the lattice of the parent phase may go through a rapid sequence of intermediate structures and then a propagation (like a strain wave) brings out a martensite plate. The atomic configuration of the embryo goes through the sequence of states by thermal fluctuations. The sequence of intermediate states is the reaction path and involves a free-energy barrier.

A spectrum of embryos of different potencies is assumed to exist. On quenching to the transformation

temperature, the free energy for nucleation drops sufficiently so that some of the embryos find themselves over the barrier. Such embryos spontaneously grow and account for the athermal transformation. Some of the embryos having smaller potency may be thermally activated to cross the free energy barrier and this gives rise to the isothermal transformation.

Machlin and Cohen⁶ studied the isothermal transformation that follows the burst in Fe - 29.5 Ni alloy. Assuming the reaction path model, they experimentally determined the relative activation energies at different temperatures. They quenched their specimens to 77°K, thereby all the embryos with free energies greater than the activation energy $W_a(77^\circ\text{K})$ would be used up in the initial burst. Immediately after prequenching to liquid nitrogen, they upquenched the specimens to various higher holding temperatures. If $N_F dF$ represents the number of embryos per unit volume having free energies between F and $F + dF$, the initial rate of nucleation \dot{N} at any higher holding temperature T is shown to be

$$\dot{N}(T) = N_F \exp \left[- \frac{W_a(T) - W_a(77^\circ\text{K})}{RT} \right]$$

$$\text{and } \dot{N}(77^\circ\text{K}) = N_F \exp k \quad 77 \text{ nuclei/c.c./sec.} \quad (1.1)$$

Since the amount of martensite is the same for all the experiments, the transformation rate is proportional to the nucleation rate.

$$\log \frac{\text{Initial Transformation rate at } T}{\text{Initial Transformation rate at } 77^{\circ}\text{K}} = \frac{W_a(T) - W_a(77^{\circ}\text{K})}{RT} \quad (1.2)$$

A plot of $W_a(T) - W_a(77^{\circ}\text{K})$ against temperature was made using the experimental transformation rates at various temperatures and the maximum rate of nucleation is estimated to be around 130°K . The calculations from the initial reaction rates did not reveal the existence of a wide spectrum of embryo potencies some of which could transform athermally on quenching in liquid nitrogen.

Mechlin and Cohen⁶ have worked out a relation between the percentage of isothermal transformation p and isothermal time t

$$p = ckT \ln \frac{t}{t_0} \quad (1.3)$$

where c is a constant and t_0 is the time required to activate one half of the most potent embryos on quenching to T . N_p is assumed to be independent of T and partitioning was neglected.

This percentage-time relation is not obeyed in their experimental curves at 200°K.

1.5 The Dislocation Model of Martensite Embryo:

Frank⁷ studied the crystallographic aspects and showed that the interface of an embryo must be a mobile link between the two phases consisting of an array of screw dislocations. The growth of martensitic plate consists of a thickening process in which the interface of screw dislocations moves ahead into the austenite. Frank's model assumes the existence of a suitable interface, and deals with only the crystallographic aspects. The problem of nucleation, or how this interface comes into being is not considered.

Assuming the existence of such an interface, Knapp and Dehlinger have developed a model which was further developed by Kaufman and Cohen⁸ to explain isothermal transformation. The martensite embryo is a thin oblate spheroid, surrounded by loops of dislocations. (Fig. 1.2) Growth of the embryo in $[1\bar{1}0]_Y$ and $[2\bar{2}5]_Y$ directions is achieved by the expansion of the dislocation loops. Growth in $[554]_Y$ direction involves creation of new dislocations. The energy for the creation of new loops is supplied by the chemical free energy change involved in the growth step. The free energy change involved in the formation of a martensite embryo is

$$\Delta w = \Delta f + \frac{3\sigma}{2c} + \frac{Ac}{r} \text{ Cal/cm}^3 \quad (1.4)$$

where σ = interfacial energy

A = elastic constant defined by $\frac{r}{c} \frac{\Delta G_E}{V}$

G_E = strain energy contribution

r = radius of the oblate spheroid of martensite embryo

c = semi thickness

It is assumed that there exists a relationship between r and c such that the embryo assumes a configuration with the minimum value of non-chemical free-energy change. This can be shown to be

$$c = \left(\frac{\sigma r}{A} \right)^{1/2} \quad (1.5)$$

With this value of c , the non-chemical free-energy term which retards the growth of the embryo is given by

$$\Delta g = \frac{3\sigma}{c} = \left(\frac{6\sigma A}{r} \right)^{1/2} \quad (1.6)$$

This quantity tends to infinity for sizes near $r = 0$.

This means that it is impossible to generate embryos from scratch. As the size of the embryo increases, the retarding force Δg diminishes. The overall free energy change ΔW of the embryo has a maximum value

$$\Delta W_* = \frac{32\pi \sigma^3 A^2}{3 \Delta f^4} \text{ Cal/particle} \quad (1.7)$$

$$\text{when } r = r_* = \frac{4 \sigma A}{\Delta f^2} \quad (1.8)$$

Spontaneous growth of the embryo by thermal fluctuations is possible only for embryos having $r \geq r_*$. The smaller embryos cannot thermally grow because their growth involves an increase in the overall free energy. For transferring the smaller embryos across the potential barrier, thermal activation is not sufficient because of the large value of ΔW_* . Even though the embryos with $r \geq r_*$ can grow to decrease ΔW , the unit growth step requires certain activation energy.

Since all the dislocation loops are coupled together, their growth cannot be considered individually. Since the embryos are very thin, the three-dimensional array of dislocations can be approximated to a dislocation loop lying in the $(225)_\gamma$ plane which follows the edge of the embryo. The energy of this equivalent loop is the surface energy of the

embryo. Therefore, it has a burger's vector $\lambda = cb/d$.

The energy of the giant loop is given by

$$W_r^l = \pi(2r\tau_l - \tau_l \lambda r^2) \quad (1.9)$$

where $\tau_l =$ line tension of the loop $= \frac{G\lambda^2}{2}$

$$\tau_l = \text{active stress on the loop}$$

$$= -\Delta f - \frac{G}{r} A$$

The chemical driving force $(-\Delta f)$ minus the strain energy expended per unit volume is the effective driving force which may be taken as the transformation stress acting on the giant loop to expand it.

Substituting the above values in eqn. (1.9),

$$W_r^l = \frac{\pi b}{d} \left[\frac{Gb}{Ad} \sigma r^2 - \tau_l r^2 c \right]$$

Substituting the numerical values for G, A, b and d,

$$W_r^l = \frac{\pi b}{d} (3.75 r^2 + \Delta f \left(\frac{\sigma}{A} \right)^{1/2} r^{5/2}) \text{ erg/loop} \quad (1.10)$$

W_r^l has a maximum value W_o^l when

$$r = r_o = \frac{9\sigma A}{f^2} \quad (1.11)$$

For embryos $r \gg r_0$, the expansion of the giant loop needs no thermal activation and the growth is cataclysmic.

The activation energy for unit growth step is given by

$$\Delta W_r^\ell = \frac{\pi b}{d} (7.5 \sigma r + 2.5 \Delta f \left(\frac{\sigma}{A}\right)^{1/2} r^{3/2}) \Delta r \quad (1.12)$$

Δr the unit displacement is taken as the burger's vector. After proper substitutions,

$$\Delta W_r^\ell = 4 \times 10^{-2} \left(\frac{\sigma}{A}\right)^{1/2} \left[3 \sigma r^{3/2} + \Delta f \left(\frac{\sigma}{A}\right)^{1/2} r^2 \right] \text{ergs.} \quad (1.13)$$

This has a maximum value ^{Fig. 3}

$$\Delta W_+^\ell = 0.11 \pi \frac{\sigma^3 A}{-\Delta f^3} \quad (1.14)$$

$$\text{when } r^{1/2} = r_+^{1/2} = \frac{2.25 (\sigma A)^{1/2}}{-\Delta f} \quad (1.15)$$

For embryos $r_* \leq r \leq r_+$, the activation energy should be taken as ΔW_+^ℓ irrespective of their size.

ΔW_r^ℓ decreases for large values of r and at

$r = r_0 = \frac{2\sigma A}{f^2}$, $\Delta W_{r_0}^\ell = 0$. For embryos with $r \gg r_0$ no thermal activation is required for growth and the growth is cataclysmic.

The embryos $r_* \leq r \leq r_0$ have to grow with the aid of thermal fluctuations to the cataclysmic size r_0 . Such embryos contribute to the isothermal transformation.

1.6 Experimental Validity of the Dislocation Model:

To explain the M_s temperature in Fe-Ni alloys, the size of the embryo has to be assumed to be 1000 Å. Richman et al.⁹ claimed to have observed embryos of about this size in thin foils of Fe - Ni alloys under electron microscope. However, from later work it appears that there is some misinterpretation. In thin foils martensite forms above the M_s temperature of bulk specimens and certain sections through the twins of martensite look similar to the martensitic embryos observed by Richman et al. No conclusive evidence is available from electron microscopic observations. However, the probability of observing such embryos under electron microscope is less than one in 10^5 if the number of pre-existing embryos is 10^7 per cm^3 .

The calculated ΔW^l was compared⁸ with the observed values of ΔW_a of Fe - Ni - Mn alloy. The value of A was taken as $500 \text{ cal/cm}^3 = 2.1 \times 10^{10} \text{ erg/cm}^3$. This was obtained from elasticity theory¹³. There is uncertainty regarding the value of σ . Treating the screw-dislocation interface as a low angle boundary, the interfacial energy is estimated

with the Read-Shockley equation as 150 erg/cm^2 . The same interface with edge dislocations will have $\sigma = 250 \text{ ergs/cm}^2$. If the interfacial energy is taken as the core energy of the screw dislocations, the elastic strain energy being taken as negligible because of the interphase nature of the boundary, then σ will be 330 erg/cm^2 . Adopting $\sigma = 160 \text{ ergs/cm}^2$ which is within the limits of uncertainty and $r = 1.8 \times 10^{-6} \text{ cm}$, good agreement is obtained between the computed and experimental activation energies over the range $80^\circ\text{K} - 180^\circ\text{K}$ in an Fe - Ni - Mn alloy. The composition of the alloy is taken to be equivalent to 25 at% Ni for ascertaining the thermodynamic data.

This model predicts the activation energy to be proportional to the driving force for transformation ($-\Delta f$). This was experimentally verified by Entwistle⁴ for Fe - Ni - Mn alloys. It was assumed that in the early stages the rate of nucleation \dot{N} is constant. Then,

$$0.002 = \dot{N} v \tau_i \quad (1.16)$$

where τ_i is the incubation period, the time required to give nucleation and v is the volume fraction of the 0.2% transform plates. v and τ_i were experimentally determined. The free energy of activation ΔW_a can be determined from the equation

$$\dot{N} = n_1 \gamma \exp - \frac{\Delta W_a}{kT} \quad (1.17)$$

where n_1 is the number of the most potent embryos per cc. There are two difficulties in comparing ΔW_a with $\Delta \frac{\ell}{r}$. A value must be assigned to n_1 to compute ΔW_a and some equivalence between nickel and manganese must be assumed to enable Δf to be calculated from the thermodynamic data available for Fe - Ni alloys. With an adapted value of $n_1 = 10^5/\text{c.c.}$, and either $N_1 = N_n$ or $2 \text{ Ni} = \text{Mn}$, then in either case the results for the alloys used by Antwislo and Shih et al show ΔW_a to be proportional to $(-\Delta f)$. However, with $n_1 = 10^7/\text{c.c.}$ (one embryo per grain), the results for different alloys fall on parallel but slightly separated lines. Considering the above mentioned uncertainties, the values of r and σ obtained by applying eqn.(1.13) to the results were found to fall in the ranges:

Ni = Mn	$r = 175 - 220\text{\AA}, \quad \sigma = 145 - 165 \text{ ergs/cm}^2$
2Ni = Mn	$r = 204 - 260\text{\AA}, \quad \sigma = 110 - 117 \text{ ergs/cm}^2$

A result of Philibert who studied the transformation in Fe - 28.17 at% Ni alloy suggests that $2\text{Ni} = \text{Mn}$ is the better assumption to make for calculating Δf . His result falls close to those of the Fe - Ni - Mn alloys only if $2\text{Ni} = \text{Mn}$.^{Fig. 4}

An indirect evidence for the Kaufman-Cohen model is given by recent studies on the kinetics of thermal stabilization. A stabilization model¹⁰ which assumes the existence

of the dislocation interface has found very good agreement with the experimental observations of the kinetics of stabilization.

To extend the theory of nucleation to explain the transformation rates at later stages of isothermal transformation, a relation between the nucleation rates and the transformation rates should be established in terms of the geometry of the martensite plate formation within a grain.

1.7 Geometry of Martensite Units:

The martensite transformation involves an increase in volume. Anisotropic strain fields are created in the matrix by the shear involved in the transformation and consequently the martensite units develop as lenticular or ellipsoidal plates. Such plates propagate until they collide with structural carriers such as grain boundaries, twin boundaries, or other martensite plates. As more and more plates form, the grain is divided into smaller and smaller compartments and therefore, the size of the plates progressively decreases. In other words, larger and larger number of nuclei will be required as the transformation progresses to give the same amount of martensite. A quantitative relation between the volume fraction and the number of plates was derived by Fisher et al¹¹. They assumed that the size of the martensite

plate is proportional to the volume fraction of untransformed austenite. They showed that

$$N = -\frac{1}{q} \left[1 - (1-v)^{1/m} \right] \quad (1.18)$$

where N is the number of plates in the volume of martensite v , q is the volume of an austenite grain and m is a shape parameter which can be taken to be the thickness to length ratio of martensite plates.

It should be noted that the treatment of Fisher et al assumes that only the grain boundaries and the existing plates are the structural barriers for the propagation of a plate. However, sometimes the plate is stopped within the grain particularly when the grain is coarse.

1.8 Autocatalysis:

The isothermal transformation rate in Fe - Ni - Mn alloys is very slow at the very initial stages of transformation, but the rate increases rapidly after a small amount of transformation. This suggests that the formation of martensite catalyses further transformation. The only model¹² that explains the experimentally observed transformation curves considers autocatalysis as an increase in the effective number of operating embryos. Assuming the number of autocatalytic embryos to be proportional to the volume

fraction of martensite formed, the following relation was derived.

$$v \exp \left(- \frac{\Delta W_a}{RT} \right) . dt = - \frac{1}{m} \frac{dV}{V^{1+\frac{1}{m}} [1 + qC + q\eta_c - qCv + v^{-1/m}]} \quad (1.19)$$

where $V = 1-v$ and c is the autocatalytic parameter which is the number of autocatalytic embryos produced during the formation of unit volume of martensite. This equation was numerically integrated with adapted values of c which give the best fit with the experimental curves. c is a function of temperature only and increases with increasing driving force. At later stages of transformation, the curves calculated from the above equation give smaller amounts of transformation than the observed amounts. This discrepancy is more at the lower temperatures of transformation. However, there is a very good agreement between the calculated and the experimental curves till an appreciable amount of martensite is formed.

2. THE EXPERIMENTAL DETAILS

2.1 Preparation of the Specimen:

The 1/2" diameter, 5" long ingot of an Fe - 30% Ni alloy made at the University of Sheffield by vacuum melting and casting was used in this investigation. The ingot was machined to remove the oxide on the surface and then swaged. The swaging is carried out in a Torrington swaging machine in eleven stages of reduction. The diameter is reduced by 0.04" in each stage, while in the last stage it is reduced by 0.035". The die used in the last stage is made in the precision shop of IIT Kanpur. After every two stages of reduction, the specimens are annealed in vacuum sealed vycor tubes for 1/2 hour at 1000°C and then furnace cooled. All the specimens were given the same treatment to ensure identical pre-history.

After swaging, the specimens are polished with an emery paper to remove any surface contamination that might have appeared during the swaging operation. A typical specimen has a diameter of 0.065" and a length of 2".

2.2 Austenitizing Treatment:

The specimens are encapsulated in vacuum in vycor tubes and are austenitized at 1100°C for 10 minutes in an

electric furnace controlled by a Leeds and Northrup temperature controller.

After austenitizing the specimens are air cooled. Air cooling is rapid enough to suppress any decomposition of austenite and slow enough to avoid the thermal strains. This material remains austenitic at room temperature. Nickel leads are then spot welded on the specimen for the sake of the electrical resistance measurements.

2.3 Electropolishing:

The electrolyte was prepared by mixing glacial acetic acid and 5% perchloric acid. The preparation of the electrolyte calls for precaution as it is a violently explosive mixture. The acetic acid is kept in a beaker which is kept in ice. After acetic acid is sufficiently cooled, perchloric acid is added in small amounts allowing sufficient time for the mixture to dissipate the heat of mixing. The most important precautions that are to be taken in making the electrolyte are

- (1) The temperature should not exceed 20°C and
- (2) No organic matter should come into contact with the solution.

Electropolishing is carried out with a stainless steel cathode. A potential of 80 volts is employed. After every 15 seconds of electropolishing, the electrolyte is allowed to cool. Each specimen is electropolished for a total time of one minute.

2.4 The Kelvin Bridge:

Kelvin bridge is a modified version of wheatstone bridge. The wheatstone bridge measures the electrical resistivity of the unknown resistance plus the resistance of the leads that connect the unknown resistance with the bridge. The resistance of the leads may cause considerable error particularly when the unknown resistance is less than 0.1 ohms. In the Kelvin bridge, the effect of the leads is rendered insignificant by putting the leads and contacts in series with high resistances in the ratio arms. This requires the use of distinct current and potential terminals for both the standard and the unknown resistance. The resistance measured corresponds only to the resistance of the specimen between the potential terminals.

A very small amount of heat is generated in the specimen due to the passage of current during measurement. To minimize the error due to heating, a press switch is incorporated in the circuit. This switch is pressed while checking the bridge balance and then only the circuit is

momentarily on. The rest of the time the circuit is off. Constant stirring of the bath helps to remove even the small amount of heat that is generated during measurement.

2.5 Experimental Procedure:

About 2 1/2 litres of methyl alcohol in a double-walled five litre Dewar flask was used as the isothermal bath. The bath was cooled to the required temperature by additions of liquid nitrogen. The bath is constantly stirred by a stirrer to ensure constant temperature in the bath. Temperature is maintained within $\pm 0.5^{\circ}\text{C}$ of the test temperature by frequent additions of small amounts of liquid nitrogen whenever the potentiometer shows a small rise in temperature. A copper-constant thermocouple (the junction is made by spot-welding) is used with a Northrup & Leeds potentiometer to measure the temperature of the bath.

In these experiments, two baths are maintained - one at -95°C and the other at the upquench temperature. After measuring the resistance of the austenite specimen in water at room temperature, it is quenched to -95°C , and the electrical resistance is measured to an accuracy of 2×10^{-6} ohms once in every 1/4 minute. After three minutes of transformation, the specimen is quickly transferred to the other isothermal bath. The resistance is

measured for about half an hour and then the specimen is upquenched to room temperature. The resistance of the specimen is again measured in water at room temperature. The room temperature readings are taken in water to remove the small amount of heat that is generated during measurement. A measurement in air shows a slightly higher value.

Maintaining two baths at the required temperatures within $\pm 0.5^{\circ}\text{C}$ simultaneously is rather difficult. Since the specimen is transferred to the upquench temperature three minutes after the start of the experiment, the second bath should be at the exact temperature three minutes after the start of the experiment. Therefore, the second bath was kept at a temperature about $1/2^{\circ}\text{C} - 3/4^{\circ}\text{C}$ lower than the required temperature at the beginning of the experiment, so that by the time the specimen was upquenched, the bath temperature came to the required temperature.

2.6 Calculation of Percentage Martensite:

R/R at 17°C that corresponds to 1% martensite is taken to be 6.8×10^{-3} for Fe - 30% Ni alloy¹². This value is used for the computation of percentage martensite from the resistivity data. Any small error in this value would only multiply the transformation rates at all temperatures and would not affect the ratios of the rates.

To find the change in electrical resistance ΔR at the test temperature, the resistance of the austenite at the test temperature had to be known. But in the alloy under investigation, about 80% of martensite forms as soon as the specimen is quenched. There is no direct method of measuring the electrical resistance of austenite at the sub-zero temperatures. The value of the temperature coefficient of resistivity α_A of pure austenite is experimentally determined by measuring resistance at various temperatures between 0°C and 35°C. The isothermal bath for this experiment is water in a dewar flask. Addition of ice and constant stirring of the bath enable a good control of temperature. The experiments on two different specimens give the values of α_A close to each other; 8.097×10^{-4} in one experiment and 8.079×10^{-4} in the other. The resistance at the test temperature is calculated on the basis of the equation

$$R_{\text{at } T^{\circ}\text{C}} = R_{17^{\circ}\text{C}} (1 + \alpha_A (T - 17)) \quad (2.1)$$

In each experiment, the specimen is upquenched to room temperature at the end of the experiment. The resistance just before the upquench and the resistance at room temperature are measured. The difference between the

resistance of austenite specimen at the test temperature (calculated on the basis of α_A and $R_{17^\circ\text{C}}$) and the resistance at the end of the experiment is ΔR at the test temperature. Thus the $\Delta R/R$ for the same amount of martensite is known at the test temperature and at the room temperature. Since the calibration reported by Naghavan corresponds to 17°C , the value of $\Delta R/R$ at the end of the experiment has to be known at 17°C to calculate the amount of martensite formed in the experiment. Since the final value of the resistance is measured at the room temperature (around 35°C), the temperature coefficient of resistivity α_m of the specimen (with martensite) has to be known to compute ΔR at 17°C . α_m is experimentally determined for four specimens. α_m versus $\Delta R/R$ at room temperature is plotted and for all other experiments α_m is read from this graph and the resistance at 17°C is then calculated. The linear relation between α_m and R/R at 35°C is given by

$$\alpha_m = 0.01019 \left(\frac{\Delta R}{R} \right)_{35^\circ\text{C}} - 0.003395 \quad (2.2)$$

Knowing $\Delta R/R$ at 17°C , the percentage of martensite formed during the experiment is computed. This martensite corresponds to $\Delta R/R$ at the test temperature. Thus $\Delta R/R$ at the test temperature that corresponds to 1% martensite is computed.

To obtain the calibration at the prequench temperature, the following method is employed. The measured resistance is plotted against time for all the experiments. The curves are extrapolated to time = 3 minutes. The resistance at prequench temperature and the test temperature just before and after the upquench are noted from the curve. To check whether any martensite formed during the upquenching, the temperature coefficient of resistance at -95°C is calculated for all the experiments.

$$\alpha_m = \frac{R_{\text{at } T} - R_{\text{at } -95}}{R_{\text{at } -95^{\circ}\text{C}} (T - (-95^{\circ}\text{C}))} \quad \text{at } t = 3 \text{ mnts.} \quad (2.3)$$

The scatter in the value of α_m is only about 10%. Therefore, it is concluded that no martensite formed during upquenching. The amount of martensite formed during the first three minutes is computed using the value of $\Delta R/R$ at the upquench temperature. Since this amount of martensite formed at -95°C , $\Delta R/R$ at -95°C that corresponds to 1% martensite is computed.

To minimise the error in the calibration of $\Delta R/R$ at various temperatures, a least square straight line is fitted with the calibration value and temperature. Using the calibration values thus obtained, percentage of martensite formed is calculated from the resistivity data of all the experiments. The typical curves are shown in figures 2.1-2

3. RESULTS AND DISCUSSION

3.1 Introduction:

Quantitative agreement between the experimental activation energies for isothermal martensite transformation and the activation energies calculated on the basis of the Kaufman and Cohen model has been shown by various investigators with the initial transformation rates of Fe - Ni - Mn alloys. Since reliable thermodynamic data are not available for Fe - Ni - Mn system, these agreements were arrived at with an assumption of some thermodynamic equivalence between Mn and Ni to calculate Δf from the available data on Fe - Ni system. Since more reliable thermodynamic data are available on Fe - Ni system, it is attempted in the present investigation to check the validity of Kaufman-Cohen model to the kinetics of isothermal transformation in Fe - 30% Ni alloy. The free energy change for the transformation can be calculated from the relation⁸

$$\begin{aligned} \Delta F^{\gamma \rightarrow \alpha'} = & - \left\{ (1-x) (1202 - 2.63 \times 10^{-3} T^2 + 1.54 \times 10^{-6} T^3) \right. \\ & + x(-3700 + 7.09 \times 10^{-4} T^2 + 3.91 \times 10^{-7} T^3) \\ & \left. + x(1-x) [3600 + 0.58 T (1 - \ln T)] \right\} \text{ cal/mol.} \end{aligned}$$

(3.1)

where x is the atomic fraction of Ni and T is the temperature $^{\circ}\text{K}$ (below 1000°K).

For obtaining the activation energies, the following equation may be used

$$\text{Nucleation rate } \dot{N} = n \gamma \exp(-\Delta W_a/kT)$$

Since the value of n is not known, the activation energy cannot be determined. However, this difficulty may be overcome by calculating the ratio of rates at two temperatures T_1 and T_2 . Then,

$$\frac{\dot{N}_1}{\dot{N}_2} = \frac{n_1 \gamma \exp(-\Delta W_{a1}/kT_1)}{n_2 \gamma \exp(-\Delta W_{a2}/kT_2)}$$

Assuming that $\frac{n_1}{n_2} = 1$

$$\frac{\dot{N}_1}{\dot{N}_2} = \exp - \left(\frac{\Delta W_{a1}}{kT_1} - \frac{\Delta W_{a2}}{kT_2} \right) \quad (3.2)$$

Since r_* varies with temperature and the operative are the ones with $r \gg r_*$, a variation of the number of embryos with temperature is a possibility. Since no information is available regarding the variation of n with temperature, it is assumed that the number of embryos

after a given amount of transformation is independent of temperature. However, the error due to the possible change in n with temperature can be minimized if we work in a temperature range where a change in temperature makes a comparatively large change in the exponential term. At temperatures near M_s , ΔT_a changes rapidly with temperature and the change in n is insignificant.

In correlating the transformation rate with the nucleation rate, the complicating factors are partitioning and autocatalysis. Both of them are functions of volume fraction of martensite formed. In the present investigation, the specimens are upquenched after three minutes of transformation at -95°C to various holding temperatures between -80 and -10°C at 10° intervals. The rates before and after the upquench vary because of the temperature change only, while the volume fraction of martensite and partitioning being the same. Since \dot{N}_1/\dot{N}_2 is found from the rates in the same specimen at the two difference temperatures, a possible variation in grain size from specimen to specimen does not affect the results.

3.2 The C-curve Behaviour:

A C-curve behaviour of the nucleation rates is observed between -95°C and -10°C . The temperature at which the maximum nucleation rate occurs is found to be

Fig 3.1

around -73°C . On the basis of the calculations made by Machlin and Cohen⁶ with the temperature dependence of the measured activation energies, the temperature of the maximum nucleation rate is around 130°K . Since the nose of the C-curve depends on the potency of the embryos, we may conclude that there is a spectrum of embryos of different potencies. After three minutes of transformation, the more potent embryos are exhausted in the transformation at -95°C and the less potent embryos remaining after 3 minutes at -95°C show the nose of the C-curve at -73°C . The Kaufman-Cohen model predicts the nose temperature of C-curve to be very sensitive to the size of the embryo.

At the temperature at which \dot{N} is maximum,

$$\frac{d\dot{N}}{dT} = -nve^{\frac{-\Delta W_n^l}{kT}} \left[\frac{1}{T} \frac{d}{dT} (\Delta W_n^l) - \frac{\Delta W_n^l}{T^2} \right] = 0$$

ie. $\frac{d}{dT} (\Delta W_n^l) = \frac{\Delta W_n^l}{T}$ at the nose temperature.

Substituting the Kaufman-Cohen expression for ΔW_r^l from eqn. (1.13)

$$T_{\max} = \frac{3 \left(\frac{\sigma A}{n} \right)^{1/2} + \Delta f}{\left[\frac{d}{dT} (\Delta f) \right]} \quad (3.3)$$

The equation (3.1) for Δf can be written by rearranging the terms as

$$\Delta f = - (F_a + F_b (1 - \ln T) T + F_c T^2 + F_d T^3) \frac{4.12 \times 10^7}{Z} \text{ ergs/c.c.} \quad (3.4)$$

where $F_a = 1202 (1-x) - 3700 x + x(1-x) 3600$

$$F_b = 0.58 x (1-x)$$

$$F_c = -2.63 \times 10^{-3} (1-x) + 7.09 \times 10^{-4} x$$

$$F_d = 1.54 \times 10^{-6} (1-x) + 3.91 \times 10^{-7} x$$

Z = Molar volume of the alloy

Substituting for Δf and $\frac{d}{dT} (\Delta f)$ in equation (3.3), it can be shown that

$$r_n = 9\sigma A / \left\{ [F_a + F_b T - F_c T^2 - 2F_d T^3] \frac{4.12 \times 10^7}{Z} \right\}^2 \quad (3.5)$$

where r_n is the size of the embryo which has the maximum probability of nucleation at temperature T . The relation between r_n and T is plotted for the alloy under investigation.

At -10°C , the value of r_n is about 460\AA (with $\sigma = 161 \text{ ergs/cm}^2$) and an embryo of size 215\AA cannot nucleate even though -10°C corresponds to the nose of the C-curve. If an

alloy contains only small embryos, it may not show any transformation because the temperatures at which the size is greater than r_* may be well below the C-curve. It is quite possible that some of the alloys which are austenitic at subzero temperatures may show isothermal transformation if their small embryos are stimulated by plastic deformation or some other means.

3.3 Activation Energy Proportional to the Driving Force:

The Kaufman and Cohen model prediction of a linear dependence of activation energy with the driving force is verified.

From equation (3.2)

$$k \ln \frac{\dot{N}_1}{\dot{N}_2} = \frac{\Delta W a_2}{T_2} - \frac{\Delta W a_1}{T_1} \quad (3.6)$$

If $\Delta W_a = a(\Delta f) + b$ where a and b are independent of temperature,

$$k \ln \frac{\dot{N}_1}{\dot{N}_2} = a \left(\frac{\Delta f_2}{T_2} - \frac{\Delta f_1}{T_1} \right) + b \left(\frac{1}{T_2} - \frac{1}{T_1} \right) \quad (3.7)$$

To avoid experimental scatter, \dot{N}_1/\dot{N}_2 is taken from the curve of \dot{N}_1/\dot{N}_2 verses temperature (fig.3.1)

$$(k \ln \frac{\dot{N}_1}{\dot{N}_2}) / (\frac{1}{T_2} - \frac{1}{T_1}) \text{ verses } (\frac{\Delta f_2}{T_2} - \frac{\Delta f_1}{T_1}) / (\frac{1}{T_2} - \frac{1}{T_1})$$

3.3
is plotted and the straight line shows that eqn. (3.7) is valid and hence the activation energy is proportional to the driving force. From the graph a and b are found and equating these values to the terms in the Kaufman-Cohen equation for \dot{W}_r eqn. (1.13),

$$a = 4 \times 10^{-2} (\frac{\sigma}{A}) r^2 = 1.742 \times 10^{-21}$$

$$b = 12 \times 10^{-2} (\frac{\sigma}{A})^{1/2} r^{3/2} = 6.236 \times 10^{-2}$$

$$\text{Putting } A = 2.09 \times 10^{10} \text{ ergs/cm}^3,$$

$$\sigma r^2 = 9.149 \times 10^{-10}$$

$$\text{and } \sigma r = 3.842 \times 10^{-4}$$

Solving these two equations,

$$r = 2.38 \times 10^{-6} \text{ cm}$$

$$\sigma = 161.4 \text{ ergs/cm}^2$$

3.4 Calculations with the Data from Machlin and Cohen:

Machlin and Cohen⁶ prequenched an Fe - 29.5% Ni alloy to liquid nitrogen temperature and then upquenched to different

holding temperatures above -70°C and measured the initial rates of transformation. They reported similar set of experiments with -70°C as the prequench temperature. In the first set of experiments, the values of $(\Delta f_2 - \Delta f_1) / (\frac{1}{T_2} - \frac{1}{T_1})$ are very close to each other. In the second set of experiments with -70°C as the prequench temperature, only three upquench temperatures were reported and a plot could not be obtained with the three points. Therefore, the following procedure is adopted to obtain the values of r . After substituting for a and b and rearranging the terms in eqn. (3.7),

$$r^{3/2} + \frac{\left(\frac{\Delta f_2}{T_2} - \frac{\Delta f_1}{T_1}\right)}{3\sigma\left(\frac{1}{T_2} - \frac{1}{T_1}\right)} r^2 - \frac{k \ln \frac{\dot{N}_1}{\dot{N}_2}}{12 \times 10^{-2} \left(\frac{\sigma}{A}\right)^{1/2} \sigma \left(\frac{1}{T_2} - \frac{1}{T_1}\right)} = 0 \quad (3.8)$$

r is obtained from this equation for several values of . For the experiments of this investigation as well as those of Machlin and Cohen, the best value of r is found to be 162 ergs/cm^2 . It is significant that the best value of r is the same for all the three sets of experiments, while r has different values. For a value of r different from 162 ergs/cm^2 , there is a systematic variation of r with

the upquench temperature. For smaller values of σ , the lower temperature gives a smaller r than the higher temperature. For higher values of σ , the trend is reversed. For example, for the experiments of the present investigation the values of r are 203 and 210 Å° for upquench rates at -80°C and -10°C respectively with a value of $\sigma = 140$ ergs/cm². But the values of r are 297 and 291 Å° respectively for upquench rates - 80°C and -10°C respectively with $\sigma = 200$ ergs/cm². However, with $\sigma = 162$ ergs/cm² variation in r for different upquench temperatures of the same set of experiments is within 1Å°. The values are tabulated below.

Prequench		r in Å°	
-95°C	3 minutes	238	
-70°C		246)	Data from Machlin and Cohen
-195°C		267)	

For a thorough verification of the model, mere proportionality between activation energy and $(-\Delta f)$ is not sufficient. The other aspects of the model have to be verified. A more crucial test for the model will be to check whether the embryos $r_* \leq r \leq r_1$ have the same activation energy of ΔW_ℓ irrespective of their size.

With the value of $\sigma = 162 \text{ ergs/cm}^2$, a calculation with eqn. (1.15) shows that r_+ at -95°C is 313 \AA which is larger than the calculated size of the embryo. If this is the case, then the activation energy should correspond to ΔW_+^l rather than ΔW_r^l . But ΔW_+^l is proportional to $1/(-\Delta f^3)$ and a proportionality of ΔW_a with $(-\Delta f)$ is not expected. The linear plot can be explained only if r_+ is shifted to a lower value during the progress of the transformation so that most of the embryos still have $r > r_+$. It is shown in the following discussion that the effect of the strains created in the matrix by the progress of the transformation is to lower the values of r_* , r_+ , r_c , and ΔW_r^l .

3.5 The Effect of Strains in the Matrix on Nucleation:

The strain produced in the matrix during the transformation may be assumed to be proportional to the volume fraction of martensite formed. It is well known fact that small amounts of plastic deformation have a stimulating effect on the embryos. Therefore, it is reasonable to propose that the strains produced by the transformation aid the energetics of the growth process of the embryos. If the strain energy due to the transformation is kv per unit volume where v the volume fraction of martensite formed and k is a proportionality

constant; then following the same arguments that were put forward in deriving the strain energy term in the eqn.

(1.4), it can be shown that the strain energy term $(\frac{c_A}{r})$ should be replaced by $(\frac{c(A-kv)}{r})$. Then equation (1.5) may be rewritten as

$$c = \left(\frac{\sigma r}{A-kv} \right)^{1/2} \quad (3.9)$$

It is metallographically observed by Raghavan¹² that the martensite plates are relatively thicker when a significant amount of martensite formed than in the early stages of the transformation. The thickness to length ratio varies from about 1/20 to 1/10 from 0 to 50% transformation. From the above consideration,

$$\frac{1}{m} = \frac{r}{c} = \left(\frac{r(A-kv)}{\sigma} \right)^{1/2} \quad (3.10)$$

It should be noted that r decreased as v increases because of partitioning.

If the above modification in the strain energy is applied, r decreases from the value given by eqn. (1.8) to r_a .

$$r_a = \frac{4\sigma(A-kv)}{\Delta f^2} \quad (3.11)$$

Then the embryos with $r_a \leq r < r_*$ which were previously inoperative become operative since they can reduce their overall free energy by growth. Then the embryos between r_a and r_* are the autocatalytic embryos. At any particular temperature, the number of embryos may be assumed to be uniformly distributed over the range r_* and r_a in the initial stages of transformation when the difference between r_* and r_a is not large.

Number of autocatalytic embryos $\propto (r_* - r_a)$

$$\propto \frac{4\sigma k}{\Delta f^2} v \quad (3.12)$$

Thus the number of autocatalytic embryos is proportional to the volume fraction of martensite formed. The dependence of the constant of proportionality on the driving force is evident. An increase in driving force brings the range $(r_* - r_a)$ to lower values of r and the distribution of the embryo size is important in determining theoretically the dependence of autocatalytic parameter on driving force. However, the distribution of embryos can be calculated from the experimental values of c at different temperatures, if this treatment is taken to be valid. The above analysis does not involve any assumption regarding the nature of the interface or the growth mechanism and therefore is more general.

However, if this treatment is applied to the Kaufman-Cohen model, another aspect of autocatalysis is evident.

The values of r_0 and r_+ are lowered by a factor of $\frac{(A-kv)}{A}$. The value of ΔW_r^l also is lowered. Since the term $\sigma/(A-kv)$ appears in the negative term and $(\sigma/(A-kv))^{1/2}$ appears in the positive term of the expression for ΔW_r^l in eqn. (1.13), the net effect of the increase in v is not much in the early stages of the transformation. For a given amount of transformation, the change in the ΔW_r^l brought about by autocatalysis should be more if Δf has a higher magnitude. This agrees with the fact that the discrepancy between the experimental transformation-time curves and a theoretical model¹² for the progress of the isothermal transformation which does not consider the lowering of activation energy by autocatalysis is more at the lower temperatures.

4. CONCLUSIONS

- 1 After 3 minutes of transformation at -95°C , the specimens were upquenched to various temperatures and the nucleation rates show a C-curve behaviour on a T-T-T diagram. The temperature at which maximum nucleation rate occurs is around -73°C .
- 2 The activation energy for nucleation is proportional to the driving force for the transformation. The values of r and σ which give best fit to the Kaufman-Cohen model are calculated.
- 3 The effect of strains produced during the transformation increases the thickness of the martensite plates at the later stages of transformation.
- 4 The proportionality between the number of autocatalytic embryos and the volume fraction of martensite formed is explained. The dependence of the autocatalytic parameter on the driving force is qualitatively explained.

- 5 If Kaufman-Cohen model is valid, autocatalysis decreases the activation energy as well as the size requirement for cataclysmic growth. The discrepancy at the later stages of transformation between the experimental transformation curves and the curves calculated on a theoretical model by Baghavan is qualitatively explained to be due to the lowering of activation energy.

TABLE I

Prequench temperature -95°C .

Upquench Temperature $^{\circ}\text{C}$	$\frac{\text{Rate at upquench temperature}}{\text{Rate at prequench temperature}}$
-10	0.31
-10	0.31
-20	0.45
-20	0.56
-30	0.68
-30	0.66
-40	0.78
-40	0.86
-50	1.04
-50	1.13
-60	1.29
-60	1.22
-70	1.38
-70	1.31
-80	1.00
-80	1.16

APPENDIX I

The following is the Fortran program for solving eqn. (3.8) for r with several values of

X = Atomic fraction of Nickel

SIG = Surface energy ergs / cm^2 .

$TRAN(I)$ = Transformation rate

$TEMP(I)$ = Temperature

$DEF(I) = \Delta f$ ergs/cc.

R = Size of the embryo $\times 10^{-6}$

NUM = Number of sets of experiments

L = Number of upquench readings +1

Subscript L refers to the prequench temperature.

TC

NODECK

DIMENSION TEMP(20), TRAN(20), F1(20), F2(20), DEF(20), FUN(20)

$X = 0.2897$

$FA = 1202. * (1. - X) - 3700. * X + X * (1. - X) * 3600.$

$FC = -2.63 * 10. ** (-3.) * (1. - X) + 7.09 * 10. ** (-4.) * X$

$FD = 1.54 * 10. ** (-6.) * (1. - X) + 3.91 * 10. ** (-7.) * X$

$Z = X * 58.71 / 8.9 + (1. - X) * 55.85 / 7.874$

DO 20 NUM=1,3

READ 9, L

FORMAT (I2)

LAST=L-1

READ 10, (TEMP(I), TRAN(I), I=1, L)

FORMAT (F6.1, F6.2)

DO 50 I=1, L

$FB = X * (1. - X) * 0.58 * (1. - ALOG(TEMP(I)))$

$DEF(I) = -((FA + TEMP(I)) * (FB + TEMP(I)) * (FC + TEMP(I) * FD))) * 4.19 * 10. ** 7) / Z$

PRINT 6, TEMP(I), DEF(I), TRAN(I)

5

FORMAT (1X, F6.1, E16.8, E16.8)

```

CONTINUE
SIG=159.0
DO 100 M=1,20
SIG=SIG+1.
Y=(SIG/8.09)**0.5
PRINT 1,SIG
FORMAT (25X,F6.1)
DO 100 I=1, LAST
SAM=3.*SIG*((1./TEMP(I))-(1./TEMP(L)))
F1(I)=(Y*((DEF(I)/TEMP(I))-(1.-DEF(L)/TEMP(L)))/SAM)*10.**(-8.)
F2(I)=(1.38*ALOG(TRAN(L)/TRAN(I)))/(4.*Y*SAM)
R=2.0
DO 7 J=1,35
R=R+0.1
FUN(I)=R***(1.5)+F1(I)*R*R-F2(I)
IF (FUN(I))15,15,7
CONTINUE
R=R-0.1
DO 18 K=1,10
R=R+0.01
FUN(I)=R***(1.5)+F1(I)*R*R-F2(I)
IF (FUN(I)) 34,34,18
CONTINUE
R=R-0.01
DO 17 K=1,10
R=R+0.001
FUN(I)=R***(1.5)+F1(I)*R*R-F2(I)
IF(FUN(I))35,35,17
CONTINUE
PRINT 5,TEMP(I),TEMP(L),F1(I),F2(I),R,FUN(I)
FORMAT (1X,2F6.1,3X,2E14.8,5X,2HB*,F6.3,5X,E16.8)
CONTINUE
STOP
END

```

REFERENCES

1. Philibert, J. and Crussard, C.; JICI 180 (1955) 39
2. Munshah, R.F. and Mehl, R.F.; Trans. AIME 197 (1953) 1251
3. Cech, R.E. and Hollomon, J.H.; Trans. AIME 197 (1953) 685
4. Entwistle, A.S.; M.I.T. Report (1961)
5. Cech, R.E. and Turnbull, D; Trans. AIME 206 (1956) 124
6. Machlin, E.S. and Cohen, M; Trans. AIME 194 (1952) 489
7. Frank, F.C.; Acta Met. 1 (1952) 15
8. Kaufman, L. and Cohen, M.; Progress in Metal Physics
Vol. 7 (1958)
9. Richman, M.H., Cohen, M. and Wilding, H.C.F.; Acta Met.
7 (1959) 819
10. Kinnsman and Shyne ; Acta Met
11. Fisher, J.C. et al; Trans. AIME 185 (1949) 691
12. Raghavan, V.; Page 30, ISI Report No. 93 (1965)
13. Ogden, H.R. and Jaffee, R.I.; Trans. AIME 191 (1951) 335

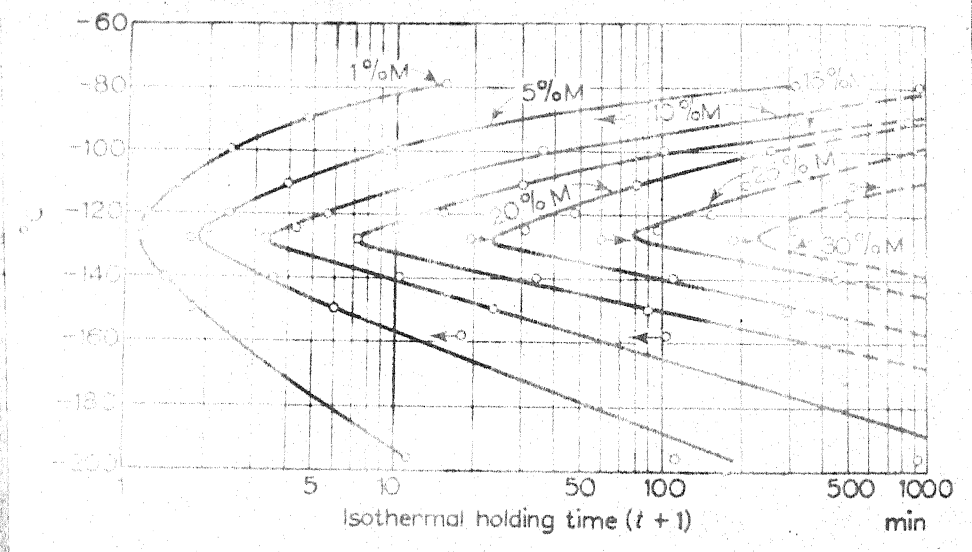


FIGURE 1.1 TTT Diagram - isothermal martensite transformation in Fe-Ni-Mn alloy.
(Cech and Holloman^{3,4})

$\pi = \Delta$ between [554]
and [110]

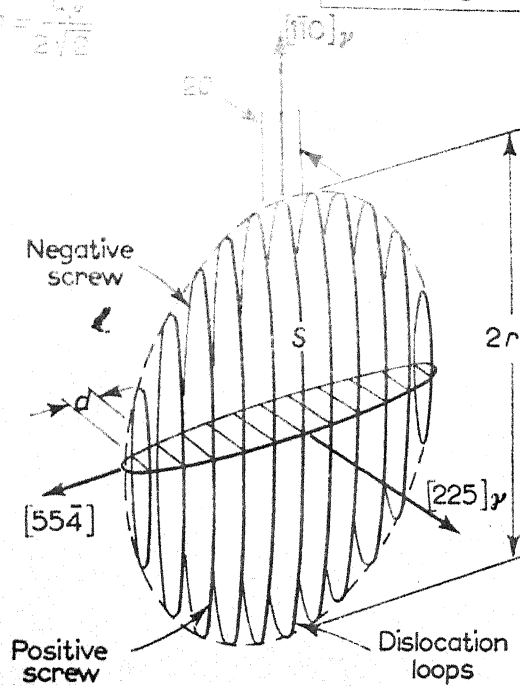


FIGURE 1.2 The Kaufman-Cohen model of martensite embryo.

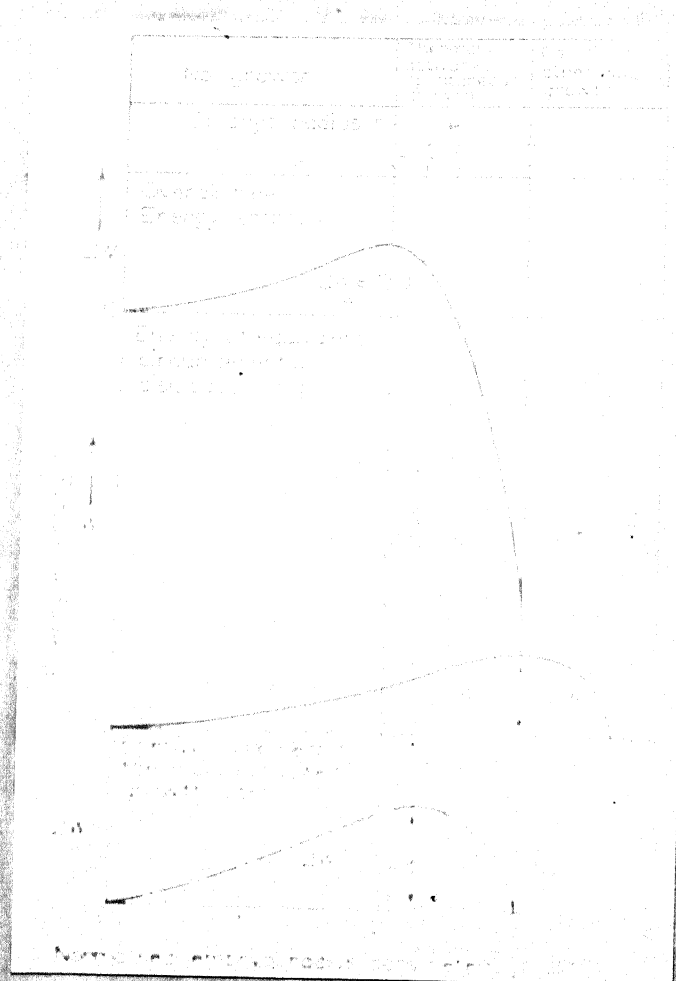
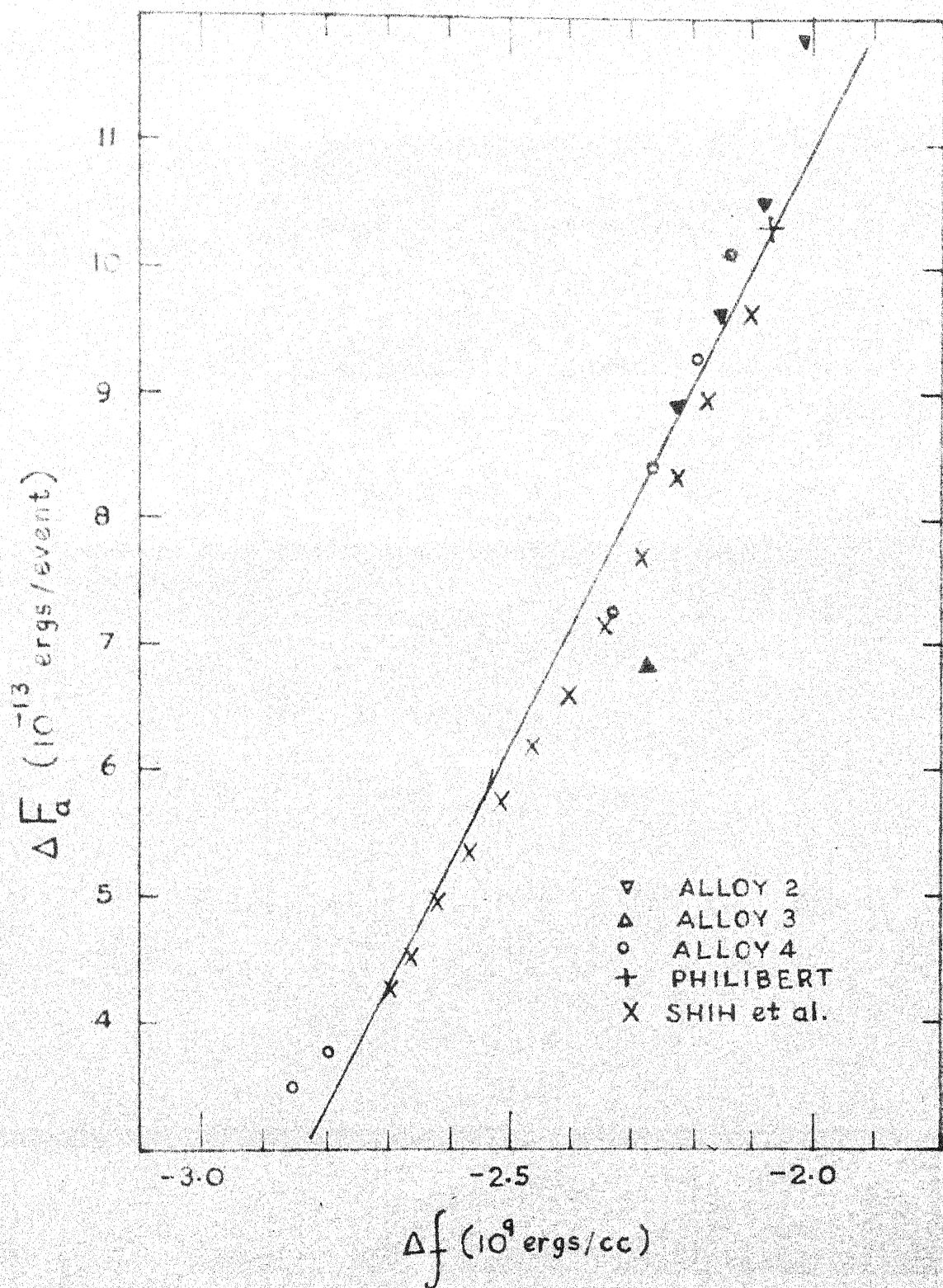


FIGURE 1.3



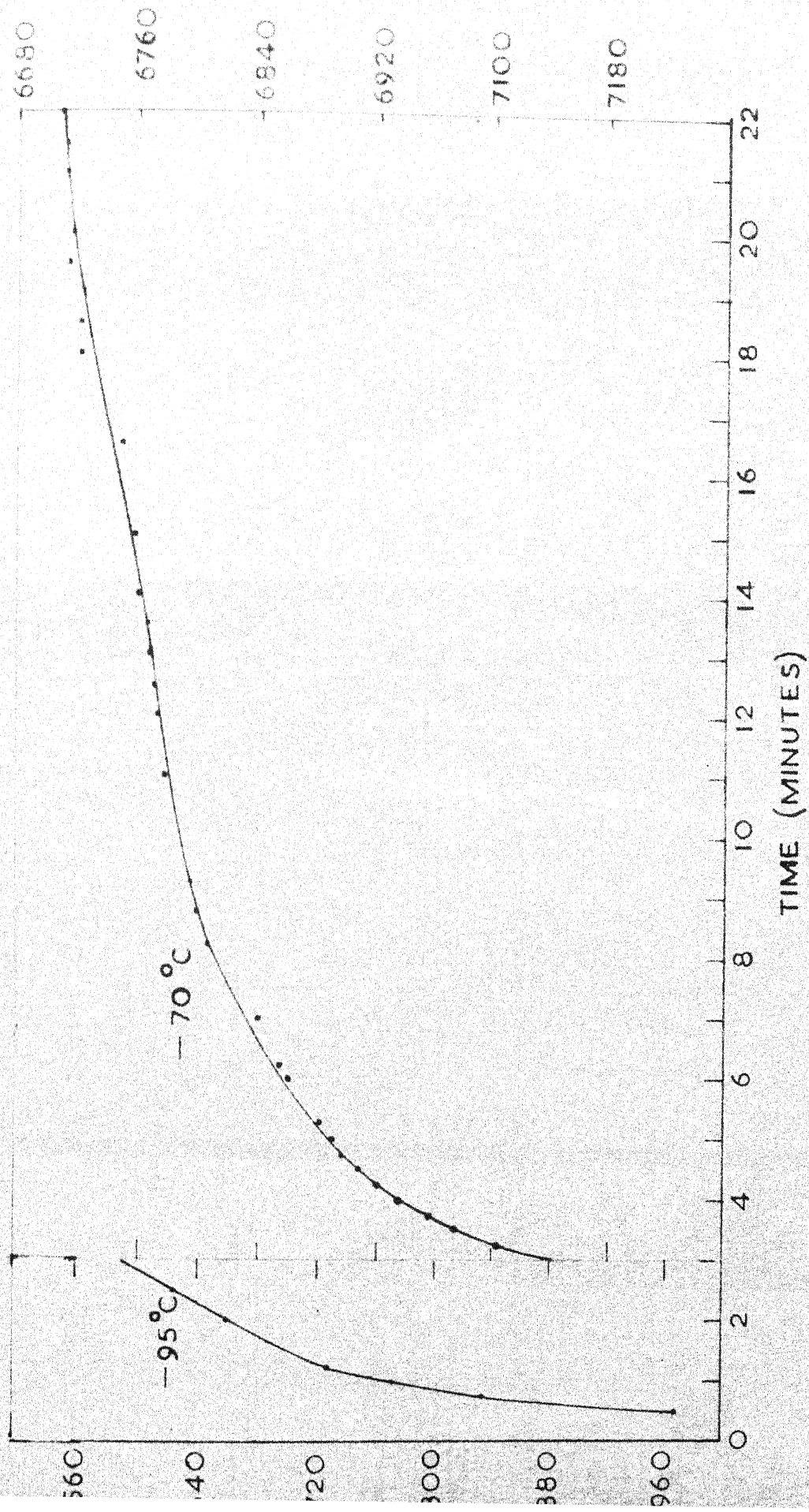


FIG. 2.1

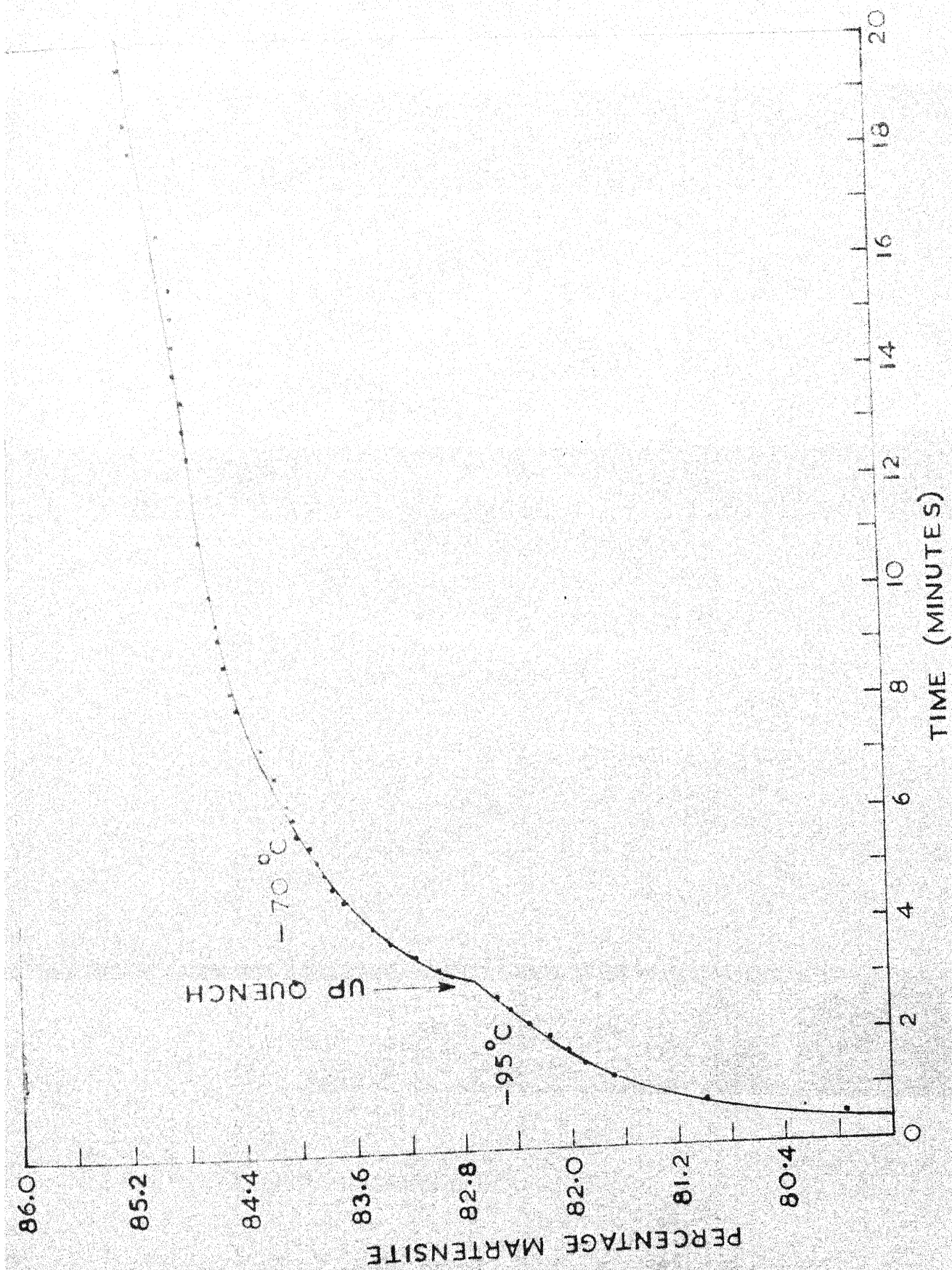


FIG. 2.2

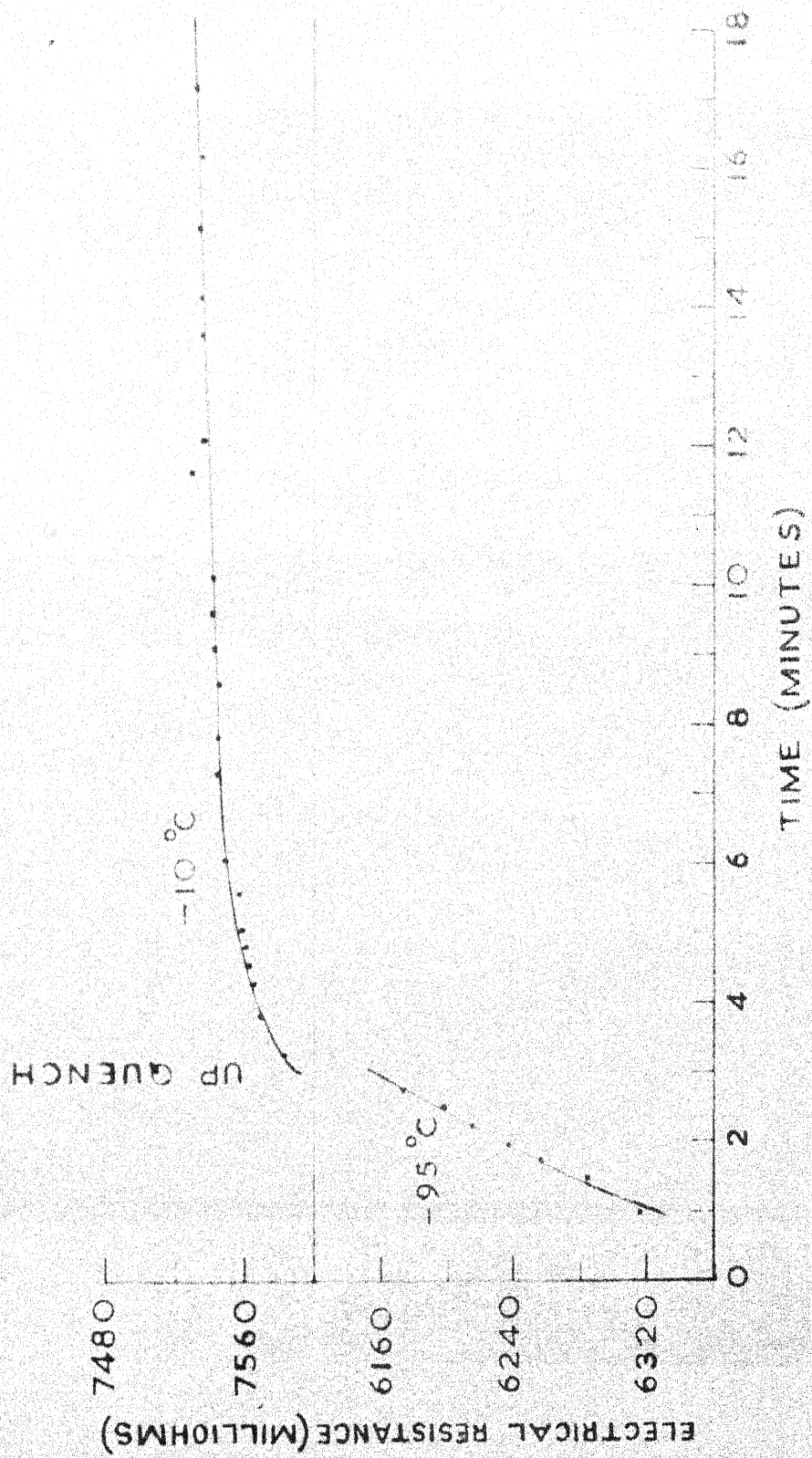


FIG. 2.3

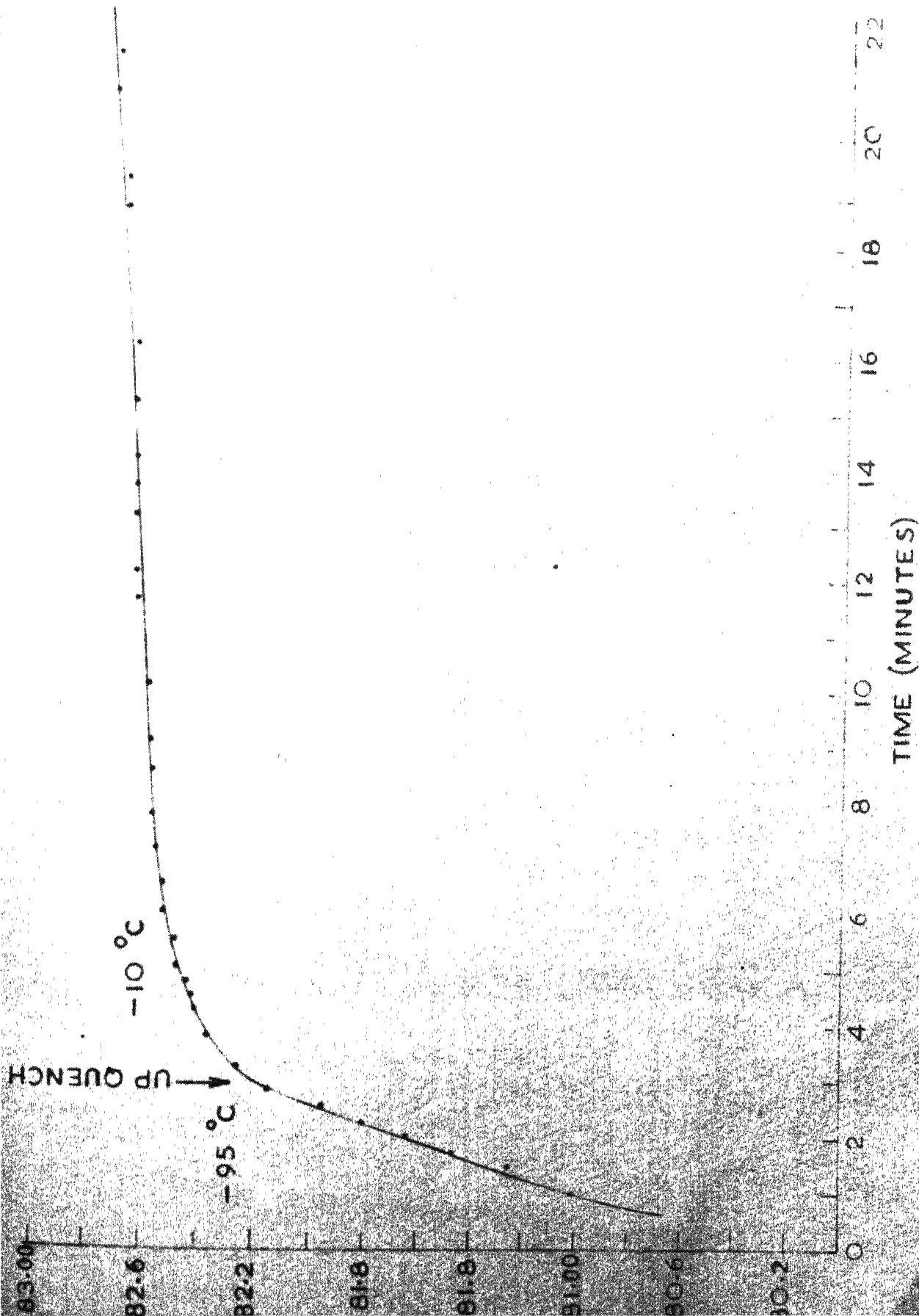
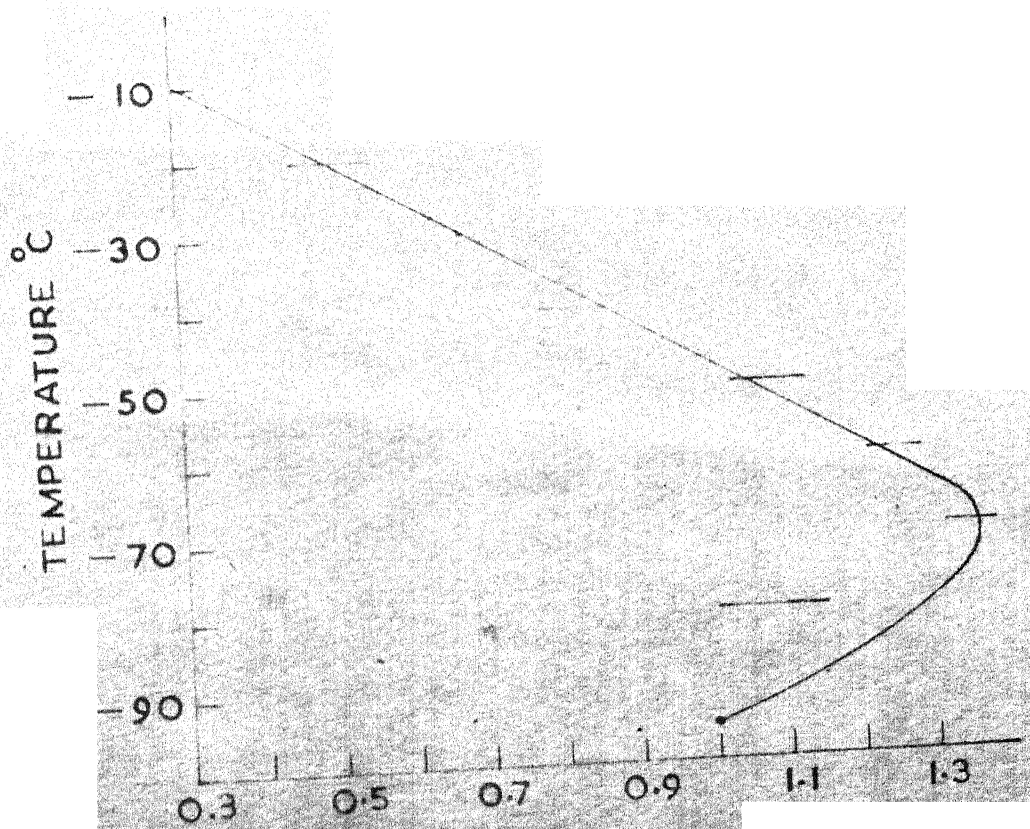


FIG. 2.4



$$\left(\frac{\dot{N}_{at} T}{\dot{N}_{at} - 95^{\circ}C} \right)$$

FIG-3.1

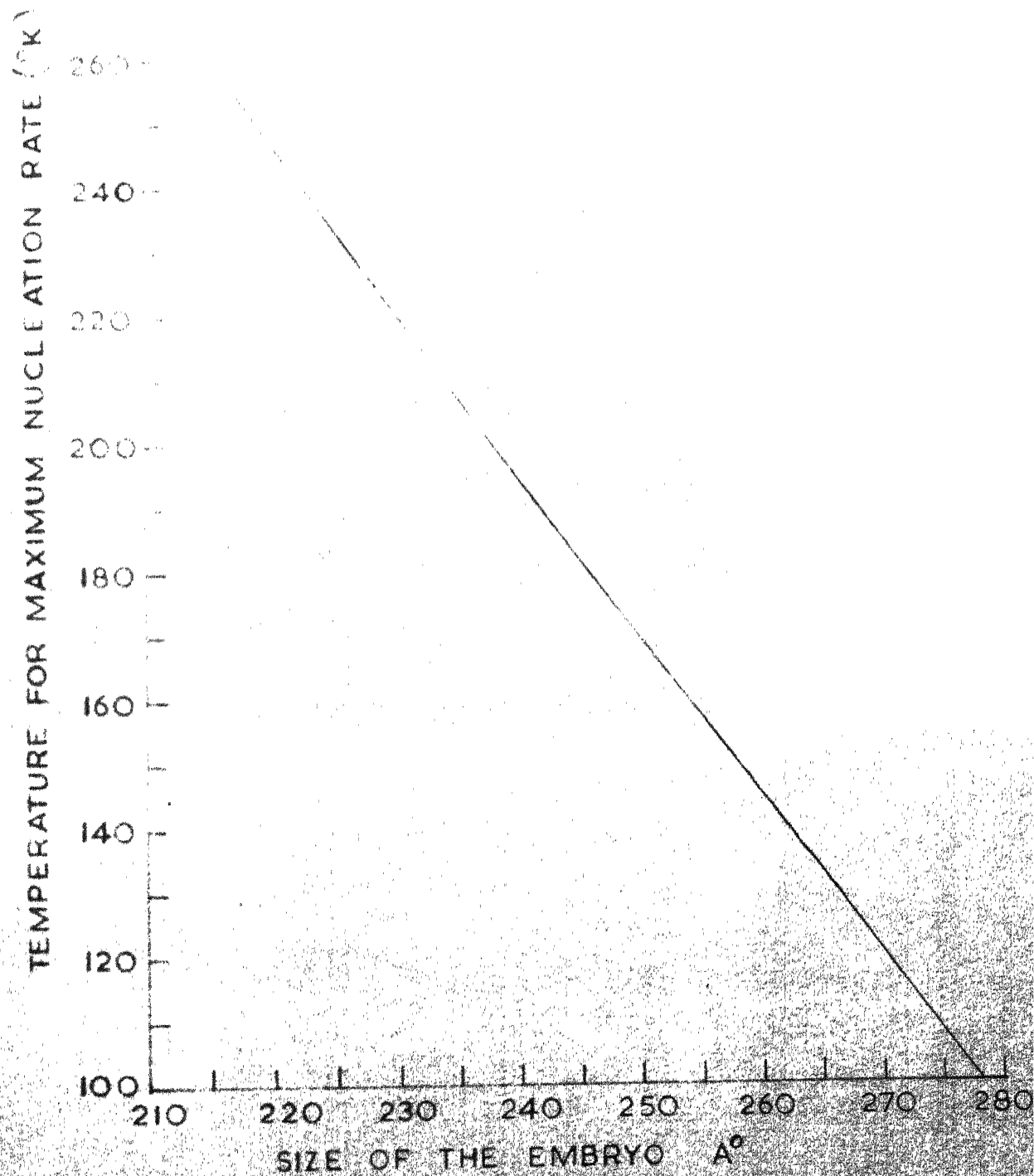


FIG. 3.2

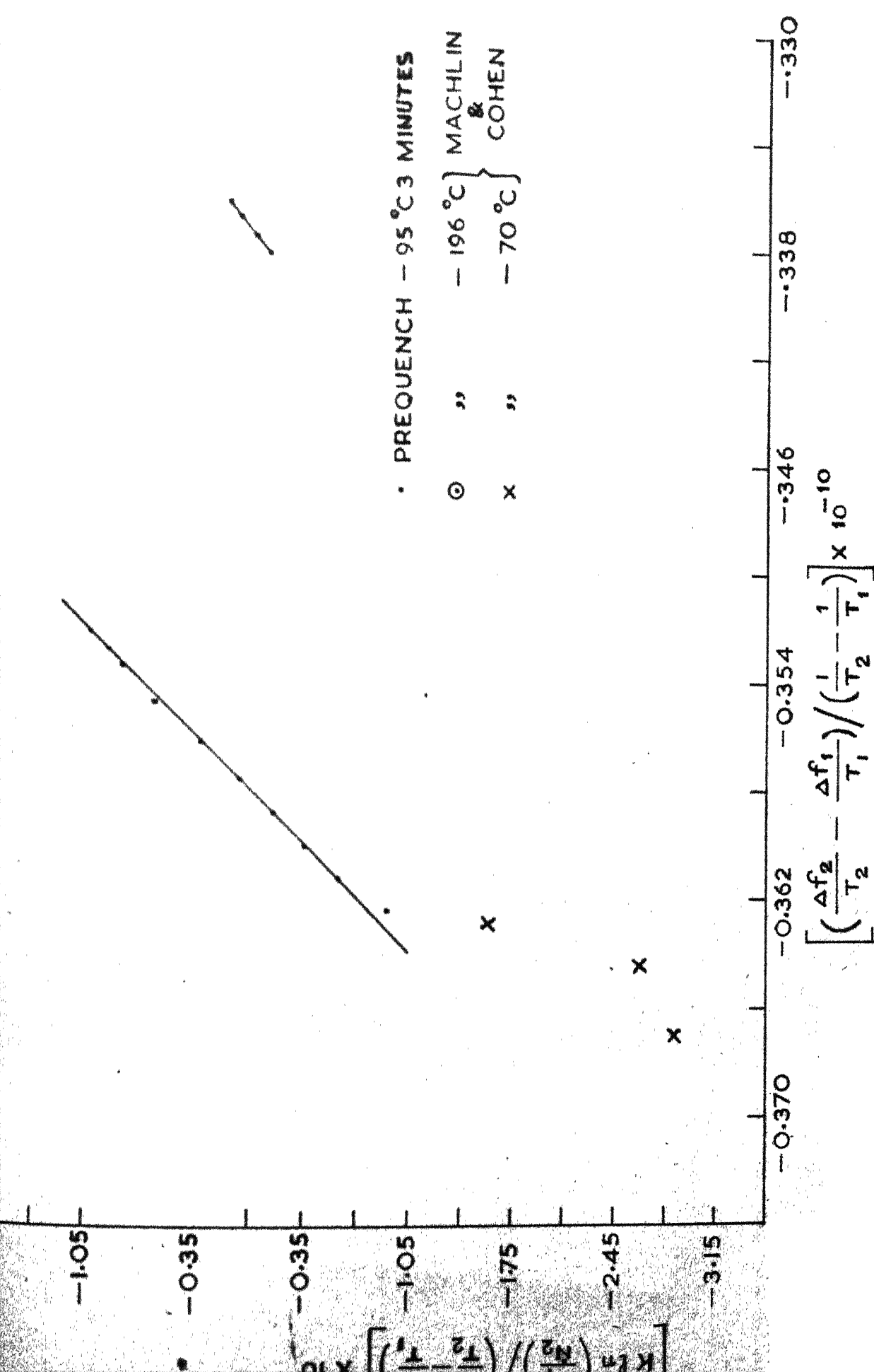


FIGURE 3.3

[illegible]

ME-1968-M-ANA-NUC.